Assessment of the impact of nanosecond plasma discharge on the combustion of methane air flames

Donato Fontanarosa[1,], Ghazanfar Mehdi[1], Maria Grazia De Giorgi[1] and Antonio Ficarella[1]*

[1]UNIVERSITA' DEL SALENTO, Department of Engineering for Innovation, 73100 Lecce, Italy

Abstract. At present, development of plasma assisted ignition and combustion is a very promising research area due to its wide applications in the field of aeronautical engines and power sector. Plasma discharge can improve the combustion because it produces large number of chemically active particles which affects the chemical reaction. Simulation is an effective tool to analyze the interaction between the plasma and the flame through the implementation of plasma-assisted combustion. This study focused on three main objectives. Initially a microscopic plasma model with detailed kinetic plasma mechanisms was developed, then the validation of these mechanisms in air/methane mixture has been performed. Finally, the effects of nano pulsed plasma discharge on combustion have been investigated. In order to accomplish the above task, two numerical tools Chemical Kinetic Solver (CHEMKIN) and Plasma Kinetic Solver (ZDPlasKin) are used. It was found that the kinetic model of plasma provides good overall agreement with experimental data and identify key processes for species (e.g. O atom) generation and decay. The results showed that with the increase of reduced electric field, active particles and intermediate species/radicals (in particular ozone) are increased. ZDPlasKin results were incorporated in CHEMKIN to investigate and compare the flame speed, thermal and chemical effect by using a GRI-Mech scheme modified with the addition of ozone reactions. It has been found that with the adding of plasma flame speed was increased up to 26% at stoichiometric ratio. The chemical heat release also showed increment at low temperatures that confirmed the combustion enhancement. Furthermore, ignition delay timings were significantly reduced with the plasma excitation.

1. Introduction

The reduction of the greenhouse gases (GHG) requires the use of low emission technologies and improved energy conversion processes. Nowadays, plasma ignited combustion is one of the most prominent and leading technology due to its growing interest in the applications of aeronautical engines [1]. Plasma discharge has the potential to enhance the combustion and flame stability by three ways: thermal effect due to Joule heating, kinetic effect with production of ions, electrons, excited species and free radicals, and the last one via transport (low temperature oxidation and fuel decomposition) [2-3]. Concerning the chemistry modification induced by plasma discharges, kinetic processes occur when electron gained additional energy and collides with gas mixture. The resulting electron impact reactions are driven by the incident energy and the cross-sectional area. Electric field strength, gas composition, gas density and the ionization degree are the important parameters to control the distribution of electron energy deposition [4].

Numerous researches focused on the definition of chemical reaction mechanisms for plasma-induced combustion enhancement. Liming et al. [5, 6] established different kinetic mechanisms and reaction paths by varying initial temperature, pressure and fuel equivalence ratios. It has been identified that plasma jet is greatly affected by air flow and igniter structure. Several research articles have been published by Central Institute for Aviation Motors (CIAM) for ignition enhancement, involving different chemical kinetic mechanisms and pathways of methane, hydrogen, ethane and syngas including vibrationally and electronically excited states [7–9]. De Giorgi et al. [10] integrated a plasma model with electron-impact excitation, dissociation, and ionization reactions into the reduced gas-phase

*Corresponding author: donato.fontanarosa@unisalento.it

radicals reaction scheme of methane combustion, to investigate the effects of plasma discharges on methane decomposition for combustion enhancement of a lean flame.

Takana et al. [11] used very simple reaction mechanism of methane – air mixture. The flow dynamics and evolution of active particles have been observed. Hongliang et al. [12] developed air discharge kinetic mechanism. Numerical simulations have been performed with repeatedly discharge in air. It has been observed that discharge frequency, reduced field strength and increasing electron concentration can increase the concentration of active particles. The modeling of low-pressure combustion in ethylene- air and methane – air in present of nanosecond pulsed discharges has been performed by Uddi et al. [13]. Fluid models of gas discharges involve the input of transport coefficients and rate coefficients, which depend on the electron energy distribution function. These coefficients can be defined from collision cross-section data by a Boltzmann equation solver [14]. Bisetti et al. [15] studied the transport of ions and electrons in CH_4 - air flames but without considering the vibrational excited states. The numerically method for calculating the transport properties of charged species in flames was discussed. Xingqian et al. [16] performed the study on the combustion of methane – oxygen by applying a direct-current and nanosecond discharge and proposed the reaction path and evolution process of active particles. Another kinetic reaction mechanism was developed by Peng Zhang et al. [17] for enhancing the plasma ignition. It was analyzed that O and its excited species have great influence on methane combustion. Previous studies mostly analyzed the effects of oxygen excited species. Recently, a numerical study by Sibo et al. [18] simulated the effects of N_2 excited species on methane combustion and analyzed the reaction path and generation of active particles. Instead, Kim et al. [19] considered the excitation states of both oxygen and nitrogen, and they retrieved that plasma assisted combustion of premixed methane - air mixture produced higher amount of NO due to excited states of N_2 when it reacts with O atom ($O + N_2^* \rightarrow NO + N$). It has been observed that O atoms have great influence on plasma combustion because a huge amount of O atom produced during nano pulse discharge.

At present, a comprehensive understanding of the hydrocarbon chemistry in presence of air and plasma actuation is still far from being fully understood due to the complexity of the plasma kinetics during the ignition in combination with the limitations of experimental measurements. Therefore, the simulation approach for developing the chemical kinetic mechanism of plasma ignition is still at the exploratory phase. However, it is a current topic in combustion research field which needed further investigations because due to lack of large amount of data which is required for a deep understanding of plasma methane/ air combustion mechanisms. Therefore, it is necessary to develop the mechanism that includes all types of reactions for plasma combustion especially involving both electronic and vibrational states, in order to analyze which species played a key role in plasma chemistry of methane-air mixture, as well as to investigate how they affect the flame behavior and the combustion performance. This study is divided in three parts:

1. The development of a ZDPlasKin-CHEMKIN method with detailed plasma kinetic mechanism;
2. Validation with experimental data;
3. Analysis of the effects of plasma discharge on flame characteristics by using nano pulse plasma discharges.

2. ZDPlasKin-CHEMKIN plasma-combustion modeling

A zero-dimensional plasma assisted combustion (PAC) simulation model is implemented to predict the temporal evolution of species and temperature. The model integrates the plasma kinetics solver ZDPlasKin [20] and the chemical kinetics solver CHEMKIN [21].

The complete detailed procedure is shown in Fig. 1. A literature survey is first performed in order to define the kinetic scheme and get the collisional cross-section data of plasma reactions (Step 1), followed by the definition of the plasma reaction simulation setting on ZDPlasKin (Step 2) consisting of the initial/boundary conditions in terms of pressure, temperature, initial mixture composition and electrical feeding, in combination with the arrangement of the chemistry file (elements, species and reactions) and the cross-section data file. Therefore, the zero-dimensional simulation of plasma is performed (Step 3), and the resulting plasma-induced mixture composition and temperature rise are used to initialize combustion simulations (Step 4). These last ones are performed (Step 5) using the CHEMKIN toolbox based on a suitable combustion kinetics scheme.

Therefore, the overall kinetic model for plasma assisted combustion is split in to two parts: plasma kinetic model and combustion kinetic model.

The first one involves the excited species quenching reactions, electron–ion recombination reactions and charge exchange reactions, the excitation and ionization electron collision reactions. The combustion chemistry involves

reactions of neutral ground-state species. A more detailed description of both kinetic schemes is provided in the following.

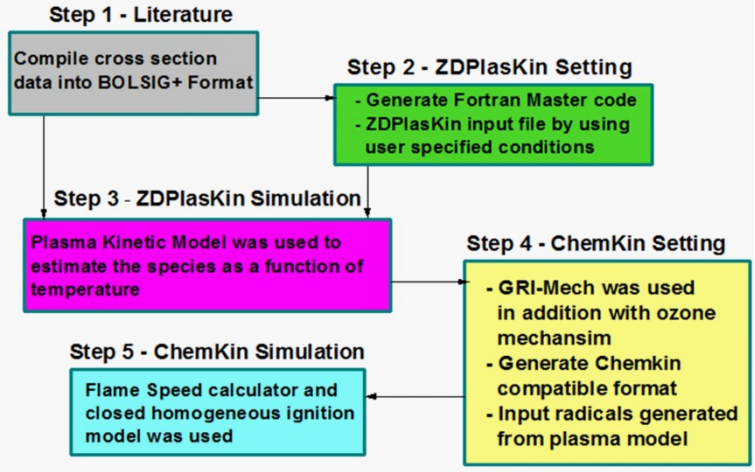

Fig.1. Proposed methodology for the analysis of plasma assisted combustion.

Table 1. Reactants, elements and intermediate species (radicals, charged and excited species) involved in detailed kinetic mechanism of plasma discharge.

Species type	**Symbol**
Reactants	CH_4, N_2, O_2
Elements	O H C N E
Radicals	H O OH HO_2 H_2O_2 CH CH_2 CH_3 CH_2O HCO HOCHO $HOCH_2O$ OCHO C_3H_3 CH_2OH CH_3O CH_3OH CH_3O_2H CH_2CO C_2H HOCO CH_3O_2 HCOH H2CC CH_3CO_3H C_2H_2 C_2H_3 C_2H_4 C_2H_5 C_2H_6 CH_3CHO CH_3CO CH_2CHO HCCO C_2O HCCOH CH_3CO_3 C_2H_5OH C_2H_5O CH_2CH_2OH CH_3CHOH $O_2C_2H_4OH$ $C_2H_5O_2H$ $C_2H_5O_2$ $C_2H_4O_2H$ C_2H_4O C_2H_3O CH_2CHOH C_3H_2 H_2CCC C_3H_6 C_3H_8 CH_3OCHO CH_3CO_2 CH_3OCO CH_2OCHO C_2H_5OCHO C_2H_5OCO CH_2CH_2OCHO $CH_3CHOCHO$ NH_3 NH_2 NH NNH N_2H_3 N_2H_2 N_2H_3 N_2H_4 N_2H_2 CN HCN H_2CN HCNN NO N_2O NO_2 NO_3 N_2O_5
Charged species	H^+ C^+ H_2^+ H^- CH^+ CH_2^+ CH_4^+ CH_3^+ CH_4^+ HCO^+ $H3O^+$ $C_2H_3O^+$ CH_5O^+ OH^- CO_3^- CHO_2^- CHO_3^- N^+ N_2^+ N_3^+ N_4^+ O^+ O_2^+ O_4^+ O^- O_2^- O_3^- O_4^- NO^+ N_2O^+ NO^- N_2O^- NO_2^- NO_3^- O_2^+ E
Excited species	C_3H_2(SING) C_3H_2(C) C_3H_4(P) C_3H_4(A) C_3H_4(C) C_3H_5(A) C_3H_5(S) C_3H_5(T) C_3H_6(C) C_3H_7(N) C_3H_7(I) OH* CH* CH_4(V24) CH_4(V13) N_2(A`1) N_2(A3) N_2(C3) N_2(V3) N_2(V1) N_2(B3) N_2(V2)) N_2(V4) N_2(V7) N_2(V5) N(2D) N_2(V6) N_2(V8) O_2(V1) N(2P) O_2(V2) O(1D) O_2(V3) O_2(B1) O_2(4.5EV) O_2(V4) O_2(A1) O(1S)

2.1 Plasma kinetic model.

High energy electron impact reactions have a significant influence on the combustion process, due to the ionization, excitation and decomposition of neutral molecules. In plasma system, electron interaction with neutral molecules significantly enhances the concentration of vibrational and electronically excited states. The reaction mechanism involves the dissociative and recombination reactions, electronically and vibrationally excited species, relaxation reactions and charged transfer reactions, three body recombination reactions concluded from the past mechanisms where available.

The mechanism consists of 161 species and 1382 reactions including both gas-phase and electron impact reactions: it has been built by extending the N_2-O_2 mixture scheme [22][23] with reactions from [24] for CH_4-H_2-O_2 mixture and

reactions from [25] for the mixture CH_4-H_2-N_2. The complete list of reactants, elements and species is shown in Table 1. Thus, for modeling the plasma discharge it is necessary to conclude the rate coefficients of electron impact reactions. Reaction rate depends upon the collision cross section of interaction and availability of electron energy. Cross sectional data for electron impact reactions taken from LXCat database [26]. For the present model, a zero-dimensional plasma kinetic solver (ZDPlasKin) incorporated with Boltzmann equation solver (BOLSIG+) for calculating the time evolution of species.

2.2 Combustion kinetic model.

The kinetic modeling of methane/air combustion was performed using a detailed chemical kinetic scheme, a data set of thermo-chemical properties, and a dataset of transport properties. The kinetic reaction mechanism used for the combustion simulation in CHEMKIN a combination of the GRI-Mech v3.08 and the set of reactions for ozone shown in Table 2 [27]. It involves 342 reactions (most of them reversible) and 54 species. These reactions include decomposition and formation reactions of ozone, oxidation reactions by ozone, and production of HO_2. The direct reaction of ozone with methane was also included in the mechanism. Details of this kinetic modeling are given in [27]. The reaction of ozone with H_2O, CH_3, N, and NO, was also included. Reactions involving excited species were not included in the present scheme.

Table.2.Sub mechanism of ozone chemical reactions included in GRI-Mech.Reaction rate coefficients$k_r = A_r T^{\beta_r} exp(-E_a/(RT))$. Units:$A_r$, cm·moles·s·K; β_r, dimensionless;E_a, J/mol.

Reaction		A_r	β_r	E_a
GM1	$O_3 + N_2 \rightarrow O_2 + O + N_2$	4.00E+14	0.0	22667
GM2	$O_2 + O + N_2 \rightarrow O_3 + N_2$	1.60E+14	-0.4	-1391
GM3	$O_3 + O_2 \rightarrow O_2 + O + O_2$	1.54E+14	0.0	23064
GM4	$O_2 + O + O_2 \rightarrow O_3 + O2$	3.26E+19	-2.1	0
GM5	$O_3 + O_3 \rightarrow O2 + O + O_3$	4.40E+14	0.0	23064
GM6	$O_2 + O + O_3 \rightarrow O_3 + O_3$	1.67E+15	-0.5	-1391
GM7	$O_3 + H \rightleftharpoons O_2 + OH$	8.43E+13	0.0	934
GM8	$O_3 + O \rightleftharpoons O_2 + O_2$	4.82E+12	0.0	4094
GM9	$O_3 + OH \rightleftharpoons O_2 + HO_2$	1.85E+11	0.0	831
GM10	$O_3 + HO_2 \rightleftharpoons O_2 + OH + O_2$	6.02E+9	0.0	938
GM11	$O_3 + H2O \rightleftharpoons O_2 + H_2O_2$	6.62E+1	0.0	0
GM12	$O_3 + CH3 \rightleftharpoons O_2 + CH_3O$	3.07E+12	0.0	417
GM13	$O_3 + NO \rightleftharpoons O_2 + NO2$	8.4E+11	0.0	2603
GM14	$O_3 + N \rightleftharpoons O2 + NO$	6.03E+7	0.0	0
GM15	$O_3 + H \rightleftharpoons O + HO_2$	4.52E+11	0.0	0
GM16	$O_3 + H2 \rightleftharpoons OH + HO_2$	6.00E+10	0.0	19840
GM17	$O_3 + CH4 \rightleftharpoons CH3O + HO_2$	8.131E+10	0.0	15280

3. Validation of Kinetic Mechanism in air and air/methane plasma.

The plasma kinetic model was validated using the experiments in [28], in which the main purpose was to investigate the role of O atom in presence of plasma discharge in air and $CH_4/O_2/$ mixture as a function of time by using nanosecond pulse discharge. A single pulse discharge was applied to the methane-air mixture: it was modelled as Gaussian shape pulse of the reduce electric field EN=E/n (where E is the electric field, n is the gas number density), with the amplitude of 289 Td and FWHM equal to the pulse duration of 25 ns. The plasma discharge was applied to a mixture with the equivalence ratio of 1 and pure air (O_2 + 3.76 N_2), at 8000 Pa and 300 K were used respectively. ZDPlasKin was used to validate the developed mechanism by considering the above experimental conditions. The numerical kinetic model showed a good agreement with experimental results of O atom molar fraction for both air and methane air mixture at same equivalence ratio, as shown in Fig. 2.

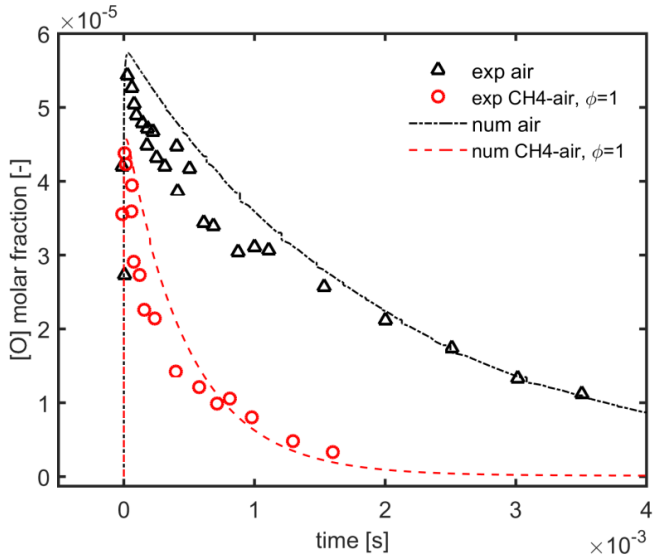

Fig. 2. Validation studies: Temporal evolution of predicted vs measured [28]O Atom with air and methane-air mixture at 300 k and 8000 Pa.

It has been analyzed that there are two primary reactions, which participated in the formation of O atoms. One is electron impact dissociation of oxygen molecule ($E + O_2 \rightarrow E + O + O$) and the second one is given by electronic excitation of nitrogen reacts with oxygen ($N_2(A3) + O_2 \rightarrow O + O + N_2$). It has been observed from Fig. 2 that the decay rate of oxygen atom in the methane/air mixture is comparatively higher than the pure air. The loss of O atoms in methane/ air mixture is due to their reactions with CH_3 radicals and H atoms, produced during methane dissociation. In presence of methane, the key reactions that consumed O are shown in Table 3.

Table.3. List of the relevant gas-phase reactions involving the O atom consumption in the methane-air mixture during plasma actuation. Rate constant k_r are in cm·molecules·s·K.

	Reaction	k_r
PM1	O+H2<=>H+OH	3.870E+04
PM2	O+HO2<=>OH+O2	2.000E+13
PM3	O+H2O2<=>OH+HO2	9.630E+06
PM4	O+CH<=>H+CO	5.700E+13
PM5	O+CH2<=>H+HCO	8.000E+13
PM6	O+CH2(S)<=>H2+CO	1.500E+13
PM7	O+CH2(S)<=>H+HCO	1.500E+13
PM8	O+CH3<=>H+CH2O	5.060E+13
PM9	O+CH4<=>OH+CH3	1.020E+09
PM10	O+CO(+M)<=>CO2(+M)	1.800E+10

4. Two-step modeling approach of the plasma assisted combustion.

Numerical modeling has been performed to analyze the kinetics effects of the main species in the mixture and the thermal and chemical effects of combustion, due to the nanosecond pulsed discharge into a typical DBD tube or parallel plate reactor. Commercially available 0-D ZDPlasKin solver was coupled with CHEMKIN software. In this study the mixture of $CH_4/O_2/N_2$ was used as an initial reactant. The equivalence ratio of mixture was 1. The temperature and pressure were 300 K and 1 atm, respectively. A DBD reactor similar to the one used for the validation case was supposed to be used: therefore, the same single Gaussian shape pulse of EN ignited the mixture, with same 25 ns FWHM. Three different amplitude were considered, i.e. 190 Td, 195 Td and 200 Td, corresponding to three

different NRP plasma actuation configurations. ZDPlasKin computations were performed in order to investigate the plasma discharge process up to 1 s after the pulse peak.

During the discharge process, energy is transferred to the neutral particles and various chemical reactions occurred such as ionization, excitation, dissociation and recombination of electron ion as shown in Fig 3. As a result, many active particles are produced which plays a key role to enhance the combustion [16]. Besides this, the temperature of unburned mixture was also increased from 300 K to 345.6 K due to the heat addition through plasma discharge.

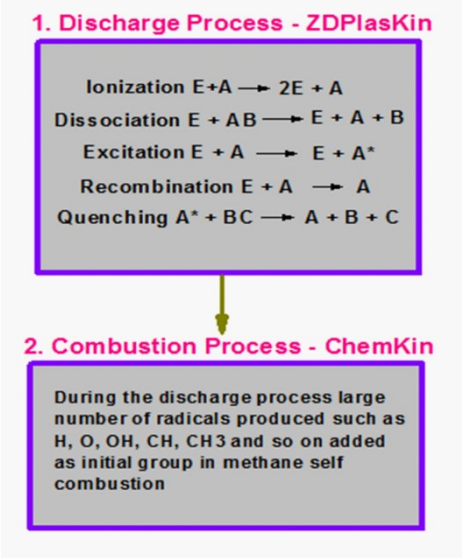

Fig. 3. Logic of the two-step modeling approach involved in plasma assisted combustion

Chemical reactions of methane/air mixture were greatly improved and accelerated by the plasma production of intermediate species like H, O, OH, CH_3, and CH. The reactant molar fraction of intermediate species is presented in Table 4. Therefore, the results (free radicals/intermediate species) produced from ZDPlasKin were incorporated in CHEMKIN to investigate and compare the flame speed, ignition delay timings, thermal and chemical effect of both classical GRI-Mech scheme and one given by the modified scheme with the addition of ozone reactions previously described. Figure 4 shows the temporal evolution of concentrations of hydrogen species. It was observed that with the increase of reduced electric field E_N, mole fraction of H atom is significantly increased. The main reactions, which are responsible for the production of H atom, are ($OH+H_2= H_2O+H$) and ($O+H_2=OH+H$).
In Fig. 5, it has been found that with the rise of E_N, concentration of OH particles initially has much higher concentrations but a smaller lifetime. At each reduced electric field OH concentration initially greatly increased and then, after a certain amount of time, it significantly reduced. The main OH reactions, which enhance the plasma-combustion process, are ($HO_2+H=2OH$), ($H+O_2=OH+O$) and ($O+H_2= OH + H$).

Table 4. Reactant mole fraction of Intermediate/radicals species used in CHEMKIN.

Species	Mole Fraction
O	9.53E-3
H	3.874E-3
OH	2.425E-3
CH	2.5587E-5
CH_3	4.04E-3

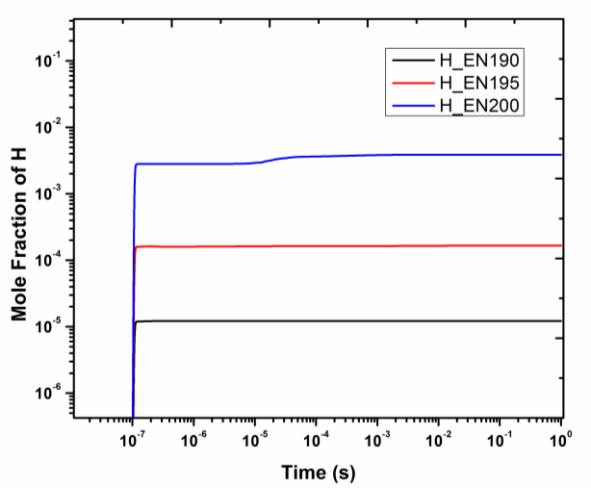

Fig. 4. Temporal evolution of H concentration at E_N= 190 Td (black solid line), E_N= 195 Td (red solid line) and E_N= 200Td (blue solid line).

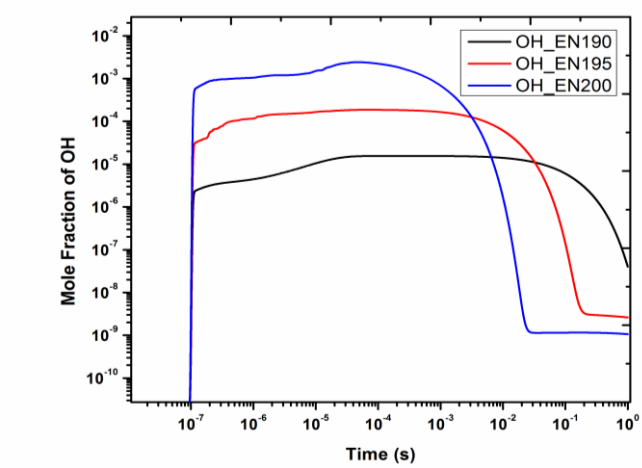

Fig. 5. Temporal evolution of OH concentration at E_N= 190 Td (black solid line), E_N= 195 Td (red solid line) and E_N= 200Td (blue solid line).

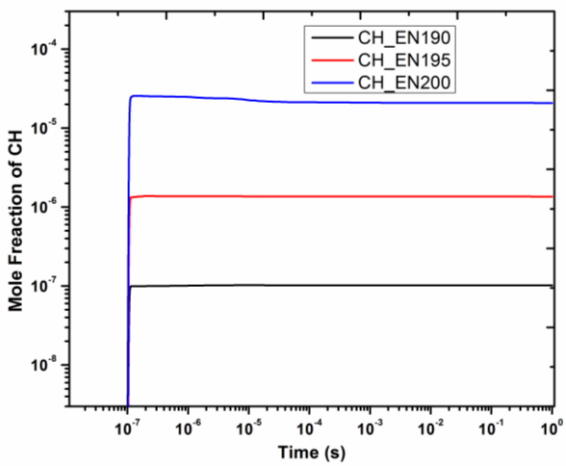

Fig. 6. Temporal evolution of CH concentration at E_N= 190 Td (black solid line), E_N= 195 Td (red solid line) and E_N= 200Td (blue solid line).

As evinced in Fig. 6, the reduced electric field has great impact on the CH specie. The mole faction of CH is greatly improved with E_N, due to the enhancement of the methane dissociation. As shown in Fig. 7, increasing the reduced electric field the same trend was observed also for CH_3. Looking to the temporal evolution of CH_3, initially it is increased due to the decomposition of methane/air plasma reaction and then slightly decreased.

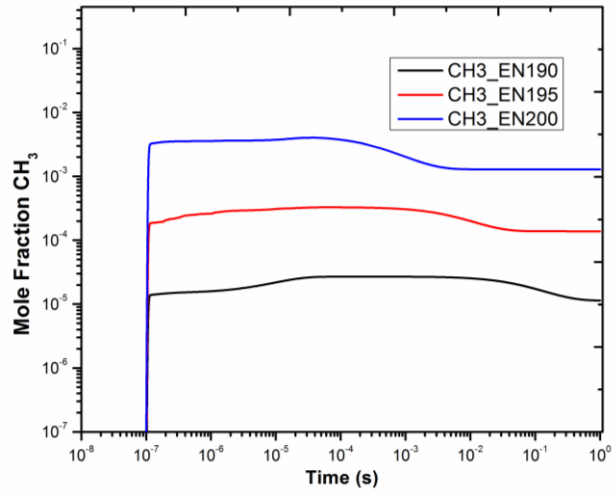

Fig. 7. Temporal evolution of CH_3concentrationat E_N= 190 Td (black solid line), E_N= 195 Td (red solid line) and E_N= 200Td (blue solid line).

The concentration and decay process of O atom is also largely increased by the rise of E_N because of the ionization of air molecules as shown in Fig.8. Furthermore, the electron impact dissociation of oxygen molecule ($E + O_2 \rightarrow E + O + O$) played important role to enhance the concentration of O atom. At first, it was increased due to the decomposition of mixture and then utilized in other reactions to form intermediate species.

NO formation is one of the most important parameters for the performance of combustion. It is produced when nitrogen reacts with air during the high temperature and very harmful for the environment. It has been observed from Fig. 9 that initially NO formation was increased with the E_N values but later decreased significantly because it was utilized in other reactions. Zeldovich reactions are the dominant source for the formation of NO. Key reactions are ($N_2 + O \rightarrow NO + N$) and ($N + O_2 \rightarrow O + NO$). It has been seen in Fig. 10 that with the increase of reduced electric field, the ozone formation is increased, because during the plasma discharge oxygen molecule reacts with O and rapidly produced ozone and it has higher impact at the 200Td.

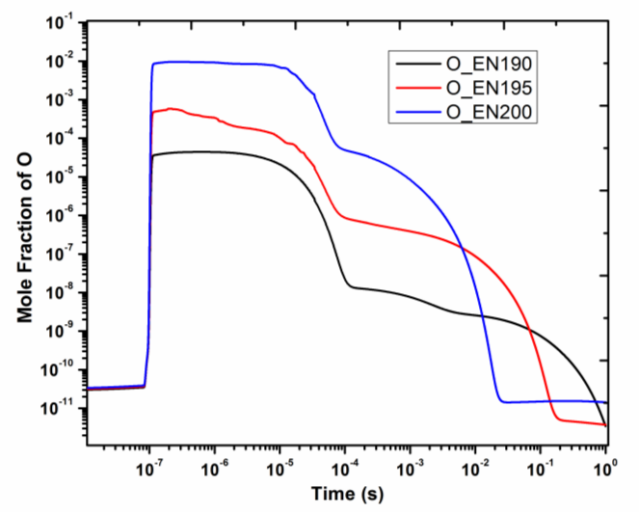

Fig. 8. Temporal evolution of O atom concentration at E_N= 190 Td (black solid line), E_N= 195 Td (red solid line) and E_N= 200Td (blue solid line).

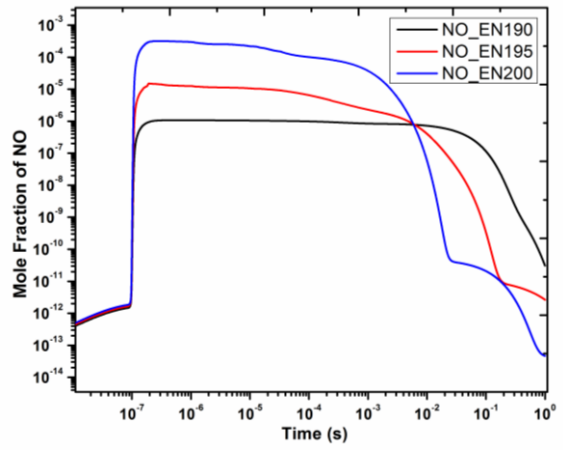

Fig. 9. Temporal evolution of NO concentration at E_N= 190 Td (black solid line), E_N= 195 Td (red solid line) and E_N= 200Td (blue solid line).

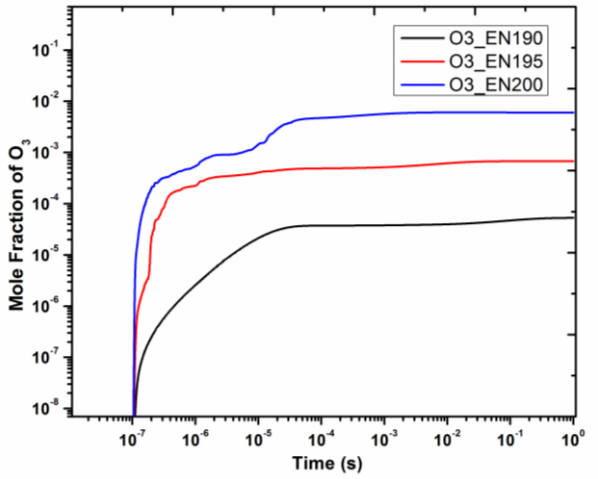

Fig. 10. Temporal evolution of O_3concentration at E_N= 190 Td (black solid line), E_N= 195 Td (red solid line) and E_N= 200Td (blue solid line).

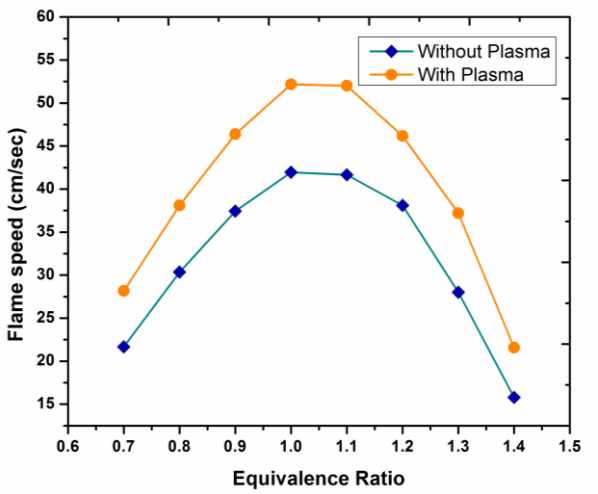

Fig. 11. Flame speed propagation by varying equivalence ratio: comparison between the clean case (blue solid line with diamond markers) and the plasma-actuated case at E_N= 200Td (orange solid line with circle markers).

Furthermore, past studies proved that ozone has potential to enhance the combustion process. Ombrello et al. [29] reported that with the addition of ozone in the air-propane combustion, flame speed was increased up to 8 %. Therefore, the ozone reactions taken from [27] accompanied with the intermediate species produced from discharge process was introduced into CHEMKIN to study the effects on the combustion process. Finally, the analysis with or without the plasma discharge was performed in the flame region.

The charged and excited particles, predicted by the ZDPasKin were excluded from the consideration and the gas mixture was assumed to consist of initial neutral species and atoms and radicals produced during the discharge and in its afterglow. The densities of atoms and radicals were used further as input parameters to simulate ignition in CHEMKIN.

Figure 11 shows the comparison of flame speed with different equivalence ratios. It has been observed that plasma discharge significantly increased the flame speed as compared with non-thermal plasma combustion because of the reduction of chemical characteristic time, which is responsible to enhance the combustion process. At stoichiometric conditions, the increment of about 26% was observed in flame speed at the maximum tested reduced electrical field, equal to 200 Td.

It has been observed and confirmed from Fig. 12, that net chemical heat production is slightly increased with the adding of plasma in the combustion process if the initial mixture temperature is in the range 1400-1700 K. The maximum chemical heat release in presence of plasma actuation was retrieved at 1600 K, which was higher than the one estimated for the baseline test case (i.e. without plasma actuation) at 1800 K. The main reason is the addition of energy coupled due to plasma discharge. The higher values of heat released significantly improved the whole reaction mechanism and as a result flame speed was improved.

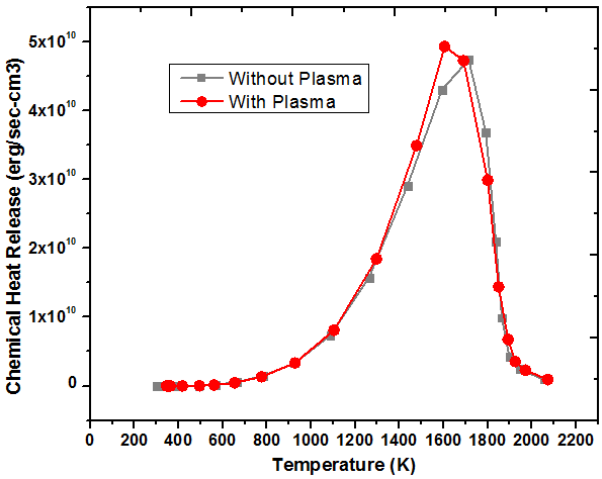

Fig.12. Chemical heat released as a function of the temperature: comparison between the clean case (gray solid line with square markers) and the plasma-actuated case at E_N= 200Td (red solid line with circle markers).

Furthermore, 0-D closed homogeneous reactor model was used to analyze the ignition delay timings at different initial mixture temperature and pressure equal to 1 atm. Two important parameters were set, temperature inflection point and the maximum OH species concentration. The ignition time was computed on the basis of maximum concentration of OH species. A comparative ignition study has been performed with or without the plasma excitation.

It was observed from Fig. 13, that under stoichiometric condition and initial temperature equal to 1500 K, plasma methane - air mixture at E_N=200 Td significantly reduced the ignition delay timings as compared with the case without plasma excitation. It indicated that the plasma excitation noticeably promoted the chemical reaction, which ultimately produced the enhancement in the combustion process. The main reason is the conversion of electron energy into bond energy of intermediate/radicals' species through the various chemical processes. Finally, during the ignition process, the bond energy of intermediate species is transformed into internal energy. The parametric measurement of ignition delay timings by considering OH peak concentration values has been carried out within various temperature ranges as shown in Fig. 14. At 1500 K the decrease of the ignition delay time due to the plasma discharge is very significant, then as the temperature increases the ignition time at OH peak is reduced slowly for plasma assisted combustion, but still it has huge difference with plasma excitation.

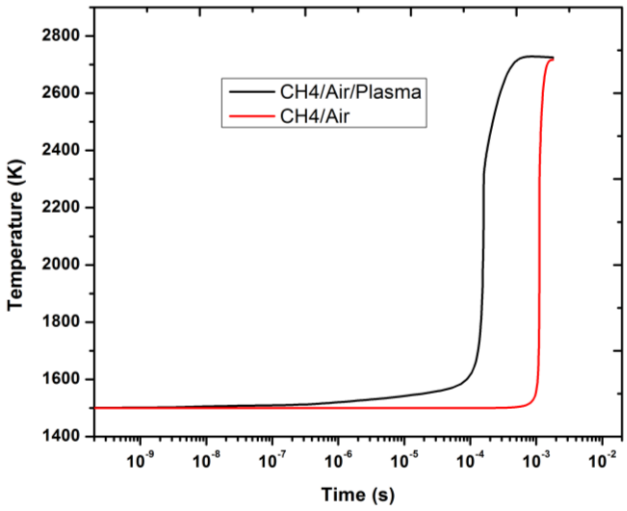

Fig. 13. Temporal temperature evolution for the baseline case (red solid line) without plasma and the plasma assisted combustion case at E_N=200 Td (black solid line) and stoichiometric condition and initial temperature 1500 K.

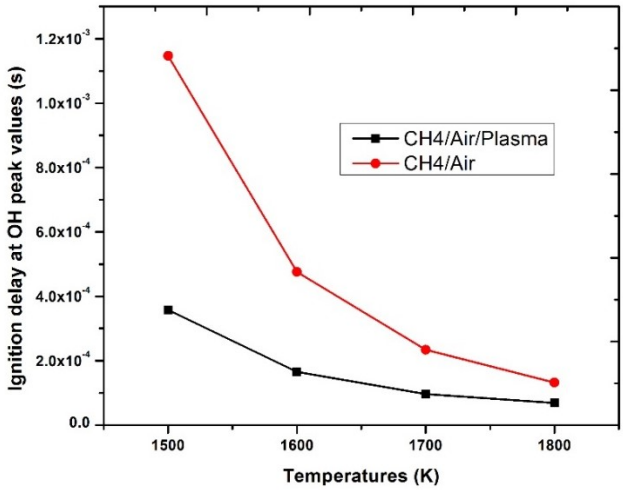

Fig. 14. Ignition delay timings by considering OH peak values with various temperature ranges

5. CONCLUSION

This study focused on the assessment of the impact of nanosecond plasma discharge on the combustion of methane-air flame. Initially a detailed microscopic kinetic mechanism was developed, then its validation was performed by comparison with experimental data of species concentrations under nano pulsed plasma discharges in a methane/air mixture. It has been found that the numerical results were in good agreement with experimental study. Finally, the effects of plasma discharge on combustion have been investigated. In order to achieve the above task, the chemical kinetic solvers, ZDPlasKin and CHEMKIN, have been used. In particular, ZDPlasKin was used to analyze the discharge process and quantify the effects of reduced electric field on the production of active particles and intermediate species/radicals. It is observed that with the increase of reduced electric field, active particles and free radicals were significantly produced leading to the enhancement of the combustion process. Results obtained from ZDPlasKin were incorporated in CHEMKIN to investigate and compare the flame speed, thermal and chemical effect predicted with the newly developed plasma scheme. It has been found that with the adding of plasma flame speed was increased up to 26% at stoichiometric ratio as compared with the case without plasma. The chemical heat release also showed a slight increment that confirmed the combustion enhancement. Furthermore, ignition delay timings were also significantly reduced with plasma excitation.

ACKNOWLEDGMENTS

This project received funding from the Clean Sky 2 Joint Undertaking (JU) under grant agreement No. 831881. The JU receives support from the European Union's Horizon 2020 research and innovation program and the Clean Sky 2 JU members other than the Union.

Nomenclature

GHC	Greenhouse gases
CIAM	Institute for Aviation Motors
NRPD	Nanosecond Repetitively Pulsed Discharge
DC	Direct Current
PAC	Plasma Assisted Combustion
NTP	Non-Thermal Plasma

REFERENCES

1. D.Q. Huang, J.L. Yu, S.B, High Voltage Eng. **44 (9)**, 3068–3075, (2018).
2. M.G. De Giorgi, A. Sciolti, S. Campilongo, A. Ficarella, Energies, **10 (3)**, art. no. 334, (2017).
3. A. Sciolti, E. Pescini, S. Campilongo, G. Di Lecce, Energy **126**, 689-706, (2016).
4. A. C. DeFilippo, J. Y. Chen, Combustion and Flame, **72**, 38–48, (2016).
5. L.M. He, W.T. Qi, B.B. Zhao, High Voltage Eng. **41 (6),**2030–2036, (2015).
6. B.B. Zhao, L.M. He, Y. Shen, High Voltage Eng. **32 (5)**, 1171–1174, (2013).
7. A .Starik, A .Sharipov, Phys. Chem. Chem. Phys. **13**, 16424–16436, (2011).
8. A .S. Sharipov, A .M. Starik, J. Phys. Chem. A. **116,**8444–8454, (2012).
9. A .M. Starik, A .S. Sharipov, J. Phys. D. Appl. Phys. **43**, 245501, (2010).
10. M.G. De Giorgi, A. Ficarella, D. Fontanarosa, E. Pescini, A. Suma, Energies, **13 (6)**, art. no. 1452, (2020).
11. H. Takana, Y. Tanaka, H. Nishiyama, J. Explor. Front. Phys. **97 (1)**, 25001.1–25001.4, (2012).
12. H.L. Du, L.M. He, W. Ding, High Voltage Eng. **36 (8),**2041–2046,(2010).
13. M Uddi, N Jiang, I V Adamovich and W R Lempert, J. Phys. D: Appl. Phys. **42,**075205 (18pp), (2009).
14. G.J.M. Hagelaar, L.C. Pitchford, Plasma Sources Sci. Technol. **14,** 722–733, (2005).
15. F. Bisetti, M. El Morsli, Combust.Flame**159**, 3518–3521, (2012).
16. X.Q. Mao, Aric Rousso, Q. Chen, AIAA Aerospace Sciences Meeting, (2018).
17. P. Zhang, Y.J. Hong, S.Z. Shen, High Voltage Eng. **40 (7),**2125–2132,(2014).
18. Sibo Wang⋆, Jinlu Yu⋆, Chemical Physics Letters **730,**399–406,(2019).
19. W. Kim, H. Do, M.G. Mungal, M. Cappelli, Proceedings of Combustion Institute **31,** 3319-3326, (2007).
20. S. Pancheshnyi, B. Eismann, G.J.M. Hagelaar, L.C. Pitchford, available at: http://www.zdplaskin.laplace.univ-tlse.fr , 2008.
21. A.E. Lutz , R.J. Kee , J.A. Miller , SENKIN: A FOR- TRAN Program for Predicting Homogeneous Gas Phase Chemical Kinetics with Sensitivity Analysis , Sandia National Laboratories, Report No. SAND87-8248 (1988).
22. M. Capitelli , C.M. Ferreira , B.F. Gordiets , A.I. Osipov, Springer, (2000).
23. A. Flitti, and S. Pancheshnyi, The European Physical Journal Applied Physics **45.2**), 21001 (2009).
24. X.Mao, A. Rousso, Q. Chen, Y. Ju, Proc. Combust. Inst. **37**, (2019).
25. X. Mao, Q. Chen, C. Guo, Energy Conversion and Management, **200,** 112018, (2019).
26. A.C. DeFilippo, Ph.D. Thesis. University of California, Berkeley (2013).
27. F. Halter,*,† P. Higelin,† and P. Dagaut, Energy Fuels, **25**, 2909–2916, (2011).
28. M. Uddi, N. Jiang, E. Mintusov, I.V Adamovich, W.R. Lempert, Proc. Combust. Inst **32**, 929–936, (2009).
29. T. Ombrello, S. H. Won, Y. Ju, S. Williams, Combust. Flame, **157 (10),** 1906–1915, (2010).